Published in IET Communications
Received on 25th January 2008
Revised on 4th August 2008
doi: 10.1049/iet-com:20080058

ISSN 1751-8628

Impacts of impulse-based ultra-wideband data links on cooperative wireless *ad hoc* networks

S. Zhu K.K. Leung A.G. Constantinides

Communications and Signal Processing Group, Department of Electrical and Electronic Engineering, Imperial College, London SW7 2BT, UK
E-mail: s.zhu@ic.ac.uk

Abstract: The recently permitted unlicenced use of the regulated ultra-wideband (UWB) radio spectrum (regulated first by the US FCC in 2002 and subsequently by the standardisation bodies of EU and other major countries) provides wireless *ad hoc* networks a cheap and promising air-interface technology for their adopted wireless data links, thus offering the potential to greatly boost their applications. The impacts of such UWB data links, mainly the more likely adopted impulse-based UWB data links for low data rate applications, on the extensively developed cooperative wireless *ad hoc* networks are investigated. First, the authors investigate the diversity order of data transfer of each impulse-based UWB data link working in a corresponding fading channel, and give an approximate relationship between the diversity order and the channel model parameters (here the Saleh–Valenzuela model parameters); Secondly, the authors develop efficient cooperative and decentralised diversity schemes that can utilise the widely spread and independently distributed multiple paths of the fading UWB channels. Performance analysis and simulation studies show that proposed decentralised cooperative beamforming schemes can achieve full diversity and are more efficient than their decentralised cooperative routing counterparts.

1 Introduction

Wireless *ad hoc* networks and their cooperative transmission strategies developed very fast in recent years [1–3], and are now being further boosted by the recently permitted unlicenced use of the regulated ultra-wideband (UWB) radio spectrum (regulated first by the US FCC in 2002 and, subsequently, by the standardisation bodies of EU and other major countries) as it provides a cheap and promising air-interface technology for the adopted wireless data links [4–7]. Because of their importance in the UWB-linked cooperative wireless *ad hoc* network design, in this paper, we investigate the impacts of such UWB data links, mainly the more likely adopted impulse-based UWB data links for low data rate applications, on the extensively developed cooperative wireless *ad hoc* networks. Our work focuses on two important issues: how is the diversity order of data transfer of each impulse-based UWB data link working in the corresponding fading channel with respect to the channel model parameters, for instance the Saleh–Valenzuela model parameters? Taking the three-node relay network as an example, what changes must be undertaken in the cooperative transmission strategies when adopting the impulse-based UWB data links?

With regard to the diversity order of data transfer of each impulse-based UWB data link working in the corresponding fading channel, we know that it relates to the detection method adopted in the UWB data link and the fading property of the UWB channels. For the impulse-based UWB data link, coherent detection is the best detection. Although many complexity-reduced detection algorithms, for examples the ones in [8, 9], have been proposed to avoid high complexity, with correspondingly improving techniques such as the multi-symbol detection techniques

these complexity-reduced detection algorithms can very closely approach the coherent detection in performance, especially in the diversity order. Hence, it is reasonable to analyse the coherent detection in the investigation of the diversity order. Further, with coherent detection, the diversity order of data transfer is determined only by the distribution of the squared norm (or total power) of the fading UWB channel. In investigating the characteristics of the UWB channels, many researchers [10–13] noticed that a fading UWB channel contains multiple delay-resolvable paths (or rays as usually called), all of which exhibit approximately Nakagami or a similar distribution in their amplitudes and can be partitioned into clusters governed by the corresponding channel model parameters. The Saleh–Valenzuela model, among similar models, is the well known basic model to mimic such channel properties and we adopt this model in our investigation as all other models could be regarded as its variates. As we have not found in the literature a paper giving the distribution of the squared norm of a UWB fading channel as well as the subsequent diversity order of data transfer with respect to the channel model parameters, in this paper, we investigate such a relationship by a combined method of analysis and simulation, and try to give an approximate formula for it.

Current cooperative transmission strategies for the three-node relay network are usually implemented in two timeslots and are usually designed for the narrowband cases [2, 3] (a recently published paper addresses the amplify-and-forward (AaF) cooperative diversity schemes on the time-hopping (TH) UWB-linked networks [14], but mainly focuses on the gains from the pulse repetition coding). The two-timeslot implementation can be described as follows. In the first timeslot, the source broadcasts data. In the second timeslot, the relay as well as the source forward data to the destination according to the designed transmission scheme. There are two possible options for the data forwarding in the second timeslot: the cooperative or opportunistic node selection, usually called the cooperative routing scheme, which requires instantaneous (block-based) route quality comparison and a carrier sensing multiple access mechanism [15–17]; and the synchronised co-channel transmission, usually called the cooperative beamforming scheme, which requires phase adjustments and power allocation [18, 19]. When adopting the impulse-based UWB data links, the UWB version of a cooperative routing scheme is similar and straightforward, whereas the unique feature of the fading UWB channels, that is, the widely spread and independently distributed multiple paths, makes the phase adjusting impossible but makes the beamforming without phase adjustments feasible and efficient, that is, it is feasible to transmit signals from two nodes to one node at a synchronised pace without severe interferences with each other. This is because the two independent channels are almost uncorrelated. This also means that for the UWB wireless *ad hoc* networks the cooperative beamforming schemes could be more efficient than their cooperative routing counterparts, as they do not need the channel information.

Our contributions in this paper can be summarised as below:

- We investigate the relationship between the diversity order of data transfer of each impulse-based UWB data link working in the corresponding fading channel and the channel model parameters (here the Saleh–Valenzuela model parameters), and give for the first time an approximate formula for it.

- We develop efficient cooperative and decentralised beamforming schemes that can utilise the widely spread and independently distributed multiple paths of the fading UWB channels. Performance analysis and simulation studies show that our proposed decentralised cooperative beamforming schemes can achieve full diversity and are more efficient than their decentralised cooperative routing counterparts.

The rest of this paper is organised as follows. Section 2 gives the network scenario under investigation and the signal model to be used. Section 3 presents the investigated relationship between the diversity order of data transfer of each impulse-based UWB data link working in the corresponding fading channel and the channel model parameters. Section 4 presents the proposed efficient cooperative and decentralised beamforming schemes that utilise the unique features of the impulse-based UWB data links. Section 5 conducts simulation studies and finally, Section 6 concludes the paper.

2 Network scenario and signal model

2.1 Network scenario

Under investigation is a UWB-linked wireless *ad hoc* network composed of a source node, a destination node and an available relay node located in between, as shown in Fig. 1. All these nodes are equipped with single-antennas and the impulse-based UWB air-interfaces. The relay works in a half-duplex manner, that is, it can either transmit or receive signal but cannot perform both at the same time. The data transfer scheme is generally implemented in two timeslots: in the first timeslot, the source broadcasts data to the

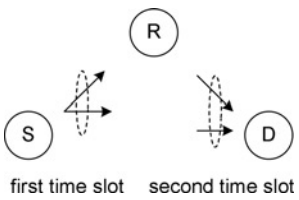

Figure 1 *UWB-linked cooperative three-node relay network: data transfer is implemented in two timeslots*

doi: 10.1049/iet-com:20080058

destination as well as the relay; in the second timeslot, the relay as well as the source forward data to the destination, according to the cooperative diversity schemes proposed later in this paper.

2.2 Impulse-based UWB data links

In an impulse-based UWB data link, every information-bearing data symbol is conveyed by N_f consecutive data-modulated ultra-short pulses, one per frame with frame duration T_f, each with unit energy and effective width $T_p \ll T_f$. The data symbol, thus, has energy N_f and lasts the duration $T_s = N_f T_f$. To ensure the resultant spectrum of the transmitted UWB signal has complied with the requirements for the unlicenced use, the pseudo-random TH or direct-sequence (DS) codes are often employed: TH codes shift the pulse positions from frame to frame at multiples of the chip duration, for example, $T_c = T_f/2 > T_p$, and DS codes modify the pulse amplitudes. Letting $c_k \in [0, 1]$ and $a_k \in [-1, 1]$ denote the TH and DS codes during the kth frame, we can represent the transmitted symbol-long waveform, if without data modulation, by

$$p_T(t) = \begin{cases} \sum_{k=0}^{N_f-1} p(t - kT_f - c_k T_c), & \text{for TH codes} \\ \sum_{k=0}^{N_f-1} a_k p(t - kT_f), & \text{for DS codes} \end{cases} \quad (1)$$

where $p(t)$ is the waveform of the ultra-short UWB pulse. If data symbols are modulated by the pulse position modulation (PPM) or pulse amplitude modulation (PAM), the transmitted signal is

$$s_{PPM}(t) = \sum_{m=0} p_T\left(t - mT_s - \frac{1 + s_m}{2}\delta\right) \quad (2)$$

or

$$s_{PAM}(t) = \sum_{m=0} s_m p_T(t - mT_s) \quad (3)$$

where $s_m \in [-1, 1]$ is the transmitted data symbol at the time index m, and $\delta > T_p$ is a small time delay used for the PPM.

Suppose the transmit power is P and the channel is $h(t)$ with the maximum effective delay spread T_h (there would be no inter-pulse interference if T_f is designed to be longer than T_h), the received signal can be represented as

$$r_{PPM}(t) = \sqrt{P}\sum_{m=0} p_R\left(t - mT_s - \frac{1 + s_m}{2}\delta\right) + w(t) \quad (4)$$

or

$$r_{PAM}(t) = \sqrt{P}\sum_{m=0} s_m p_R(t - mT_s) + w(t) \quad (5)$$

where $w(t)$ is the received zero-mean Gaussian white noise and

$$p_R(t) = p_T(t) * h(t) = \begin{cases} \sum_{k=0}^{N_f-1} p_h(t - kT_f - c_k T_c) \\ \sum_{k=0}^{N_f-1} a_k p_h(t - kT_f) \end{cases} \quad (6)$$

where

$$p_h(t) = p(t) * h(t) \quad (7)$$

Here, we only consider the case with DS codes and PAM data modulation, just for simplicity, as it is straightforward to extend the results to any other case. We also only consider the case of coherent data detection in which the channel waveform is estimated first and then used to correlate the received signal in the corresponding matched filter. This is because although various complexity-reduced detection algorithms have been proposed to avoid high complexity needed by the coherent detection, these complexity-reduced detection algorithm with the corresponding improving techniques can approach very closely the coherent detection. Thus, the received signal, after the pulse-matched filter and Nyquist rate sampler, can be written as

$$r_{m,k,j} = \int_0^{T_{sa}} r(t)p(t - mT_s - kT_f - jT_{sa})dt = s_m\sqrt{P}a_k h(jT_{sa}) + n_{m,k,j} \quad (8)$$

where $k = 0, \ldots, N_f - 1, j = 0, \ldots, (T_f/T_{sa}) - 1$, T_{sa} is the Nyquist integration and sampling interval which could be half of T_p, and $n_{m,k,j}$ is the corresponding noise item with zero-mean σ_n^2-variance Gaussian distribution. Hence, s_m can be coherently detected as follows

$$r_m = \sum_{k=0}^{N_f-1}\sum_{j=0}^{(T_f/T_{sa})-1} r_{m,k,j}a_k h(jT_{sa}) = s_m N_f\sqrt{P}\sum_{j=0}^{(T_f/T_{sa})-1}|h(jT_{sa})|^2 + \sum_{k=0}^{N_f-1}\sum_{j=0}^{(T_f/T_{sa})-1} n_{m,k,j}a_k h(jT_{sa}) \quad (9)$$

The signal-to-noise ratio (SNR) of s_m in r_m, that is, the receiver SNR of the impulse-based UWB data link, is

$$\rho = \frac{PN_f\sum_j |h(jT_{sa})|^2}{\sigma_n^2} \quad (10)$$

It should be noted that although the transmitted data symbols in the impulse-based UWB data communication are normally assumed binary, it is feasible and actually straightforward to be extended to the case where analogue values are adopted (even

for the PPM data modulation), to approach the channel capacity potential. Because of the limited space in this paper, we only consider the case with the capacity-approaching coded data symbols. This means that when the receiver SNR is higher than a value, then the transmitted corresponding capacity-approaching coded data symbols can be decoded without error.

2.3 Fading UWB channels

UWB signals, when travelling through reflective environments, usually exhibit multiple delay-resolvable paths that appear as rays in clusters [10–13]. The basic model for such UWB channels is the so-called Saleh–Valenzuela model [10], which uses five parameters m_c, λ_c, γ_c, Λ_c and Γ_c to describe these clustered rays. According to the Saleh-Valenzuela model, a UWB channel exhibits three levels of fading (by using the word 'fading' here, we wish to express the variation of the path amplitudes of the UWB channel):

- All rays have amplitudes exhibiting Nakagami-m_c distribution, where m_c is around 0.5;
- In each cluster, the rays arrive according to a Poisson distribution with the parameter λ, that is, the arrival interval between two consecutive intra-cluster rays exhibit the exponential distribution with mean $1/\lambda_c$, and their average power decays exponentially with the time constant γ_c;
- The first rays of clusters arrive according to a Poisson distribution with the parameter Λ, that is, the arrival interval between the first rays of two consecutive clusters exhibit the exponential distribution with the mean $1/\Lambda_c$, and their average power decays exponentially with the time constant Γ_c.

In such a manner, the channel is written as the sum of all these rays

$$h(t) = \sum_{l=0}^{\infty}\sum_{k=0}^{\infty} h_{l,k}\delta(t - T_l - \tau_{l,k}) \tag{11}$$

where $h_{l,k}$ refers to the amplitude of the kth ray in the lth cluster, and

$$E\{|h_{l,0}|^2\} = E\{|h_{0,0}|^2\}e^{-T_l/\Gamma_c}, \quad \Pr\{T_{l+1}|T_l\} = \Lambda_c e^{-\Lambda_c(T_{l+1}-T_l)} \tag{12}$$

$$E\{|h_{l,k}|^2\} = E\{|h_{l,0}|^2\}e^{-\tau_{l,k}/\gamma_c}, \quad \Pr\{\tau_{l,k+1}|\tau_{l,k}\} = \lambda_c e^{-\lambda_c(\tau_{l,k+1}-\tau_{l,k})} \tag{13}$$

and $|h_{l,k}|^2$ exhibits Gamma-m_c distribution with a mean of $E\{|h_{0,0}|^2\}e^{-T_l/\Gamma_c}e^{-\tau_{l,k}/\gamma_c}$.

It should be noted that considering the exponential decay of the power of the clustered rays, the channel realisations with limited but sufficiently large total number of clusters and total number of rays in each cluster have little effect on the resultant diversity order of data transfer.

2.4 Performance metrics for data transfer over fading channels

When using the capacity-approaching coded data symbols, a suitable data transfer performance measure in fading contexts is the probability of the outages in which the data link cannot support a given data rate. According to the definition in [20], the outage probability for the data transfer at a given data rate r_{ρ_o} is

$$P_{\text{out}} = \Pr\left\{C(\rho) = \frac{1}{2}\log_2(1+\rho) < r_{\rho_o} = \frac{1}{2}\log_2(1+\rho_o)\right\} = \Pr\{\rho < \rho_o\} = \Pr\left\{\frac{\rho}{\overline{\rho}} < \frac{\rho_o}{\overline{\rho}}\right\} \tag{14}$$

where C is the channel capacity, ρ_o the minimum SNR that can support the data rate r_{ρ_o} and $\overline{\rho}$ the average receiver SNR. The asymptotic outage probability (AOP) when the average receiver SNR tends to infinity can show the diversity order of data transfer in a fading channel at a high SNR region [20]

$$P_{\text{out}}^{(\text{asy})} \overset{\overline{\rho}\to\infty}{\simeq} \Omega\left(\frac{\rho_o}{\overline{\rho}}\right)^{\omega} \tag{15}$$

where ω is the diversity order and Ω the corresponding gain.

3 Diversity order of impulse-based UWB data link working in fading channel

The data transfer performance of each impulse-based UWB data link working in the corresponding fading channel is determined by the distribution of the SNR of its link receiver, or further by the distribution of the squared norm (or total power) of the fading channel. However, such a distribution is very difficult to derive. To conduct the performance analysis and simulations studies, below we first derive the average total power of a fading UWB channel when its channel model parameters are given, and then investigate the relationship between the diversity order of data transfer and the channel model parameters by a analysis and combined method of analysis and simulation.

3.1 Average total power of fading UWB channel

For a fading UWB channel with Saleh–Valenzuela model parameters m_c, λ_c, γ_c, Λ_c and Γ_c, the average power of the

doi: 10.1049/iet-com:20080058

second ray in cluster l is

$$E\{|h_{l,1}|^2\} = E\{|h_{l,0}|^2\}E\{e^{-(\tau_{l,1}/\gamma_c)}\}$$
$$= E\{|h_{l,0}|^2\}\int_0^\infty e^{-(\tau_{l,1}/\gamma_c)}\lambda_c e^{-\lambda_c\tau_{l,1}}d\tau_{l,1}$$
$$= E\{|h_{l,0}|^2\}\frac{\lambda_c\gamma_c}{1+\lambda_c\gamma_c} \quad (16)$$

Hence, the average total power of the rays in this cluster is

$$\sum_{k=0}^{+\infty}E\{|h_{l,k}|^2\} = E\{|h_{l,0}|^2\}\left[1+\frac{\lambda_c\gamma_c}{1+\lambda_c\gamma_c} + \left(\frac{\lambda_c\gamma_c}{1+\lambda_c\gamma_c}\right)^2+\cdots\right]$$
$$= E\{|h_{l,0}|^2\}(1+\lambda_c\gamma_c) \quad (17)$$

and therefore the average total power of all the rays of this fading UWB channel is

$$\sum_{l=0}^{+\infty}\sum_{k=0}^{+\infty}E\{|h_{l,k}|^2\} = E\{|h_{0,0}|^2\}(1+\lambda_c\gamma_c)(1+\Lambda_c\Gamma_c) \quad (18)$$

In practice, the total number of clusters and the total number of rays in each cluster are large but limited. Considering the exponential decay property of the power of the clustered rays, this has very little effect on the diversity order of data transfer we have obtained here.

3.2 Diversity order of data transfer over fading UWB channel

The receiver SNR of each impulse-based UWB data link working in a fading channel, according to (10), is

$$\rho = \frac{PN_f\sum_{l=0}^{\infty}\sum_{k=0}^{\infty}|h_{l,k}|^2}{\sigma_n^2} \quad (19)$$

The average receiver SNR of each UWB link, using (18), is

$$\overline{\rho} = \frac{PN_fE\{|h_{0,0}|^2\}(1+\lambda_c\gamma_c)(1+\Lambda_c\Gamma_c)}{\sigma_n^2} \quad (20)$$

Thus, the normalised receiver SNR of each UWB link is

$$\frac{\rho}{\overline{\rho}} = \frac{\sum_{l=0}^{\infty}\sum_{k=0}^{\infty}|h_{l,k}|^2/\mathrm{E}\{|h_{0,0}|^2\}}{(1+\lambda_c\gamma_c)(1+\Lambda_c\Gamma_c)} \quad (21)$$

As its probability distribution is very difficult to derive, we first consider the case for the channel that only contains one cluster of rays as follows, and then extend the results to the multi-cluster channels.

The power of the second ray in a cluster is

$$|h_{l,1}|^2 = E\{|h_{l,0}|^2\}x_{l,1}^2e^{-(\tau_{l,1}/\gamma_c)}$$
$$= E\{|h_{l,0}|^2\}x_{l,1}^2a_{l,1} \quad (22)$$

where $x_{l,1}$ exhibits a Nakagami-m_c distribution and $\tau_{l,1}$ exhibits the distribution $p(\tau) = e^{-\lambda_c\tau}$, thus $a_{l,1} = e^{-(\tau_{l,1}/\gamma_c)}$ exhibits distribution $p(a) = \lambda_c\gamma_c a^{\lambda_c\gamma_c-1}$, $0 \le a \le 1$. We can see that $a_{l,1}$ exhibits a distribution only determined by the multiplication $\lambda_c\gamma_c$, not each of them. Considering that the first ray accounts for m_c order of diversity, we therefore can assume that the diversity order of the impulse-based UWB data link working over a single-cluster channel to be $m_c[1+f(\lambda_c\gamma_c)]$. In the simulations, we noticed that $f(\lambda_c\gamma_c)$ is approximately linear and so, here, we assume it approximately as $c\lambda_c\gamma_c$. Extensive simulation results suggest that such an assumption is reasonable and feasible. Table 1 shows the simulation results on the diversity order for the data transfer over the fading single-cluster UWB channel with $m_c = 0.5$. From Table 1, we can see that the constant c is around (a little bit less than) 2, and we can obtain an approximate relationship as follows

$$\omega \simeq m_c(1+2\lambda_c\gamma_c) \quad (23)$$

This result obtained from extensive simulations shows that although the number of multiple paths in the UWB channel is very high, its corresponding diversity order of data transfer is limited and fixed, and can be known roughly by the channel model parameters.

When extending this to multi-cluster channels, we can see that theoretically the value swap between $\lambda_c\gamma_c$ and $\Lambda_c\Gamma_c$ does not change the resultant diversity order, and the diversity order only depends on the sum of them, that is, $\lambda_c\gamma_c + \Lambda_c\Gamma_c$, as shown in Table 2. From the simulation results, we can easily give the following approximate relationship between the diversity order and the channel model parameters

$$\omega \simeq m_c[1+2(\lambda_c\gamma_c+\Lambda_c\Gamma_c)] \quad (24)$$

Table 1 Diversity order of data transfer over fading single-cluster channel, $m_c = 0.5$

λ_c γ_c	ω
1.0	1.45
1.5	1.90
2.0	2.22
2.5	2.65
3.0	3.02

Table 2 Diversity order of data transfer over fading UWB channel, $m_c = 0.5$

$\lambda_c\ \gamma_c + \Lambda_c\Gamma_c$	ω
1.0	1.45
2.0	2.23
3.0	3.02

4 Efficient cooperative and decentralised diversity schemes

The received signals at the destination and the relay in the first timeslot, according to (5), are as follows

$$r_{d1}(t) = \sqrt{P}\sum_m s_m \sum_{k=0}^{N_f-1} a_k p_{h_{sd}}(t - mT_s - kT_f) + w_{d1}(t) \tag{25}$$

$$r_r(t) = \sqrt{P}\sum_m s_m \sum_{k=0}^{N_f-1} a_k p_{h_{sr}}(t - mT_s - kT_f) + w_r(t) \tag{26}$$

where subscript '$d1$' refers to 'the destination and the first timeslot', subscript 'r' refers to 'the relay', subscript 'sd' refers to 'from the source to the destination', and subscript 'sr' refers to 'from the source to the relay'. The signals are received in zero-mean Gaussian white noise, and the ultra-short UWB pulses are distorted by the UWB channels; $p_{h_{sd}}(t)$ is the received pulse distorted by channel h_{sd}, $p_{h_{sr}}(t)$ is the received pulse distorted by channel h_{sr}, and they are almost uncorrelated from each other as

$$\frac{|\int p_{h_{rd}}(t)p_{h_{sd}}(t)\mathrm{d}t|^2}{\int |p_{h_{rd}}(t)|^2\mathrm{d}t \int |p_{h_{sd}}(t)|^2\mathrm{d}t} \Rightarrow 0 \tag{27}$$

Based on these received signals, we can obtain two decision variables for the data symbol s_m, a scaled version of $s_m\sqrt{\rho_{sd}} + n_m^{(d1)}$ at the destination and a scaled verstion of $s_m\sqrt{\rho_{sr}} + n_m^{(r)}$ at the relay, where $n_m^{(d1)}$ and $n_m^{(r)}$ are corresponding zero-mean unit-variance Gaussian white noise items, and ρ_{sd} and ρ_{sr} are the corresponding link receiver SNRs.

4.1 Cooperative beamforming

Cooperative beamforming refers to the operation in which the relay and the source forward their received or original data to the destination at a synchronised pace with suitable weights, to create a combined source-destination data transfer route that is associated with the highest instantaneous (block-based) data transfer quality. Here, the synchronisation between the relay and the source can be easily achieved from the data broadcasting and reception in the first timeslot, and owing to the widely spread and independently distributed multiple paths of the fading UWB channels, such cooperative beamforming could be implemented without severe mutual suppression of the transmitted signals from different nodes.

The received signal at the destination in the second timeslot is

$$r_{d2}(t) = q_r\sqrt{P}\sum_m \tilde{s}_m^{(r)} \sum_{k=0}^{N_f-1} a_k p_{h_{rd}}(t - mT_s - kT_f) + q_s\sqrt{P}\sum_m s_m \sum_{k=0}^{N_f-1} a_k p_{h_{sd}}(t - mT_s - kT_f) + w_{d2}(t) \tag{28}$$

where subscript '$d2$' refers to 'the destination and the second timeslot'. q_r and q_s are the weights satisfying $q_r^2 + q_s^2 = 1$. The transmitted signal from the relay, if the decode-and-forward (DaF) data forwarding policy is adopted, is

$$\tilde{s}_m^{(r)} = \begin{cases} s_m, & \text{if } \rho_{sr} \geq \rho_o \\ 0, & \text{otherwise} \end{cases} \tag{29}$$

If the AaF policy is adopted, it is

$$\tilde{s}_m^{(r)} = \frac{s_m\sqrt{\rho_{sr}} + n_m^{(r)}}{\sqrt{\rho_{sr} + 1}} \tag{30}$$

As the UWB channel-distorted received pulses from the relay and the source $p_{h_{rd}}(t)$ and $p_{h_{sd}}(t)$ are almost uncorrelated, the resultant receiver SNRs of the combined source-destination data transfer route for different policies can be derived below.

4.1.1 DaF policy: The destination receives the signal from the source in the first timeslot; it also receives signals from both the relay and the source in the second timeslot. Based on these received signals, the corresponding receiver SNR of the combined source-destination data transfer route can be derived as

$$\rho = \begin{cases} (1 + q_s^2)\rho_{sd} + q_r^2\rho_{rd}, & \text{if } \rho_{sr} \geq \rho_o \\ (1 + q_s^2)\rho_{sd}, & \text{otherwise} \end{cases} \tag{31}$$

To achieve its maximum value, the best set of weights should be

$$[q_r^2 \quad q_s^2] = \begin{cases} (1\ 0), & \text{if } \rho_{sr} \geq \rho_o, \rho_{rd} > \rho_{sd} \\ (0\ 1), & \text{otherwise} \end{cases} \tag{32}$$

and with the optimum weights, the resultant receiver SNR is

$$\rho = \begin{cases} \rho_{sd} + \max(\rho_{sd}, \rho_{rd}), & \text{if } \rho_{sr} \geq \rho_o \\ 2\rho_{sd}, & \text{otherwise} \end{cases} \tag{33}$$

doi: 10.1049/iet-com:20080058

4.1.2 AaF policy: The impulse response of the matched filter in coherent detection should be a scaled version of

$$q_{\mathrm{r}}\frac{\sqrt{\rho_{\mathrm{sr}}}}{\sqrt{\rho_{\mathrm{sr}}+1}}\sum_{k=0}^{N_{\mathrm{f}}-1}a_k p_{b_{\mathrm{rd}}}(t-kT_{\mathrm{f}})+q_{\mathrm{s}}\sum_{k=0}^{N_{\mathrm{f}}-1}a_k p_{b_{\mathrm{sd}}}(t-kT_{\mathrm{f}})$$

and, hence, the corresponding receiver SNR of the combined source-destination data transfer route can be derived as

$$\begin{aligned}\rho &= \rho_{\mathrm{sd}}+\frac{(q_{\mathrm{r}}^2(\rho_{\mathrm{sr}}\rho_{\mathrm{rd}}/(\rho_{\mathrm{sr}}+1))+q_{\mathrm{s}}^2\rho_{\mathrm{sd}})^2}{\rho_{\mathrm{sr}}(q_{\mathrm{r}}^2(\rho_{\mathrm{rd}}/(\rho_{\mathrm{sr}}+1)))^2}\\ &\quad +q_{\mathrm{r}}^2(\rho_{\mathrm{sr}}\rho_{\mathrm{rd}}/(\rho_{\mathrm{sr}}+1))+q_{\mathrm{s}}^2\rho_{\mathrm{sd}}\\ &= \rho_{\mathrm{sd}}+\frac{q_{\mathrm{r}}^2(\rho_{\mathrm{sr}}\rho_{\mathrm{rd}}/(\rho_{\mathrm{sr}}+1))+q_{\mathrm{s}}^2\rho_{\mathrm{sd}}}{(\rho_{\mathrm{sr}}(q_{\mathrm{r}}^2(\rho_{\mathrm{rd}}/\rho_{\mathrm{sr}}+1))^2)}\\ &\quad /(q_{\mathrm{r}}^2(\rho_{\mathrm{sr}}\rho_{\mathrm{rd}}/(\rho_{\mathrm{sr}}+1))+q_{\mathrm{s}}^2\rho_{\mathrm{sd}})+1\end{aligned} \tag{34}$$

To achieve its maximum value, the optimum set of weights can be derived by assuming the derivatives of the resultant SNR with respect to the weights to be zeros

$$q_{\mathrm{r}}^2=\begin{cases}\dfrac{\rho_{\mathrm{sd}}(\rho_{\mathrm{sr}}\rho_{\mathrm{rd}}/(\rho_{\mathrm{sr}}+1)-\rho_{\mathrm{sd}})}{2\rho_{\mathrm{sd}}\rho_{\mathrm{sr}}(\rho_{\mathrm{rd}}/(\rho_{\mathrm{sr}}+1))^2-(\rho_{\mathrm{sr}}\rho_{\mathrm{rd}}/(\rho_{\mathrm{sr}}+1)-\rho_{\mathrm{sd}})^2}, & \text{if } \in[0,1]\\ 1, & \text{if } \notin[0,1],\ \dfrac{\rho_{\mathrm{sr}}\rho_{\mathrm{rd}}}{\rho_{\mathrm{sr}}+\rho_{\mathrm{rd}}+1}>\rho_{\mathrm{sd}}\\ 0, & \text{otherwise}\end{cases} \tag{35}$$

and with the optimum weights, the resultant receiver SNR can be calculated.

4.2 Data transfer performance of cooperative beamforming schemes with optimum weights

In the second timeslot, the case with $q_{\mathrm{r}}=1$ or $q_{\mathrm{s}}=1$ corresponds to a route selector, a special case of the cooperative beamforming. Thus, the cooperative beamforming scheme with optimum weights should be no worse than the schemes using route selectors. As the cooperative routing can achieve full diversity, the cooperative beamforming with optimum weights can achieve full diversity as well.

As the results for the AaF policy are very similar, in the following, we just give the outage probability of the cooperative beamforming scheme with the optimum weights for the DaF policy.

Theorem 1: Suppose each of the impulse-based UWB data links exhibits the data transfer AOP $\Omega(\rho_o/\overline{\rho})^{\omega}$, if the widely spread and independently distributed multipath channels are uncorrelated from each other, then the data transfer adopting the proposed cooperative beamforming scheme with optimum weights for the DaF policy has the AOP less than

$$\frac{\Omega^2}{2^{\omega-1}}\left(\frac{\rho_o}{\overline{\rho}}\right)^{2\omega}$$

Proof: See Appendix 9.1. □

This theorem demonstrates the full diversity of the proposed cooperative beamforming schemes with the optimum weights.

4.3 Decentralised implementation

The decentralised implementation of the proposed cooperative beamforming schemes depend on the weight determination or what degree of channel information can be collected at the relay and the source. Here, we consider two options: the one in which the relay knows its in-coming channel information by estimation; and the other in which the relay and the source both know nothing but that there are two nodes participating in the beamforming.

4.3.1 Option 1: The relay estimates the instantaneous (block-based) link quality of its in-coming link in the first timeslot. Based on this, we assume the weights in the second timeslot as

$$q_{\mathrm{s}}=\frac{\sqrt{2}}{2},\quad q_{\mathrm{r}}=\frac{v_{\mathrm{r}}}{C} \tag{36}$$

where v_{r} is the relative weight, and C is a constant adopted for the normalisation of weights

$$C\Rightarrow\sqrt{2E\{v_{\mathrm{r}}^2\}} \tag{37}$$

In such a manner, the average (over all blocks) transmit power remains unchanged

$$E\{q_{\mathrm{r}}^2+q_{\mathrm{s}}^2\}=1 \tag{38}$$

For the DaF policy, we may set

$$v_{\mathrm{r}}=\begin{cases}1, & \text{if } \rho_{\mathrm{sr}}\geq\rho_o\\ 0, & \text{otherwise}\end{cases} \tag{39}$$

For the AaF policy, we may set

$$v_{\mathrm{r}}=\frac{\rho_{\mathrm{sr}}}{\rho_{\mathrm{sr}}+1} \tag{40}$$

4.3.2 Option 2: In this case, the relay and the source choose the same weights as $\sqrt{2}/2$. As the results for the AaF policy are very similar, in the following, we just give the outage probability of the proposed decentralised cooperative beamforming scheme with equal weights for the DaF policy.

Theorem 2: Suppose each of the impulse-based UWB data links exhibits data transfer AOP $\Omega(\rho_o/\overline{\rho})^{\omega}$, if the widely spread and independently distributed multipath channels for different links are uncorrelated from each other, then the data transfer adopting the proposed distributed cooperative beamforming scheme with equal weights for the DaF policy has the AOP less than

$$\frac{4^{\omega}+2^{\omega}}{3^{\omega}}\Omega^2\left(\frac{\rho_o}{\overline{\rho}}\right)^{2\omega}$$

Proof: See Appendix 9.2. □

This theorem implies that even without knowing the instantaneous (block-based) data link quality the proposed distributed cooperative beamforming schemes can still achieve full diversity.

5 Simulations studies

In the simulations, we assume the following settings: the ultra-short UWB pulse has the waveform as the second derivative of the Gaussian function with an effective width of 0.7 ns; the data symbol has 16 frames, each lasts 16 pulse widths; the data symbols are modulated by the PAM; the UWB channels are produced according to IEEE Standard UWB channel CM-1 with channel model parameters (Λ, Γ, λ, γ) as (0.047, 22.61, 0.15, 12.53) and all rays in the channels exhibit a Nakagami-$m_c = 0.5$ distribution in amplitudes. This implies that the data transfer of each impulse-based UWB link over the corresponding fading channel has the AOP

$$\Omega\left(\frac{\rho_o}{\overline{\rho}}\right)^{\omega} \simeq 25\left(\frac{\rho_o}{\overline{\rho}}\right)^{3.4} \tag{41}$$

and on average two disturbed pulses by independently produced UWB channels with the above channel model parameters are almost uncorrelated, that is

$$E\left[\frac{|\int p_{b_1}(t)p_{b_2}(t)\mathrm{d}t|^2}{\int |p_{b_1}(t)|^2\mathrm{d}t \int |p_{b_2}(t)|^2\mathrm{d}t}\right] < 0.01 \tag{42}$$

Fig. 2 shows the comparison of two simulated results for the outage probability of an impulse-based UWB data link working in the corresponding fading channel: one is directly simulated, the other is simulated according to the given approximate formula. We can see that these two results match very well.

Fig. 3 shows the outage probabilities of the proposed cooperative beamforming schemes and their decentralised implementations. Here, 'DaF route' refers to the route from the source to the destination via the relay adopting the DaF

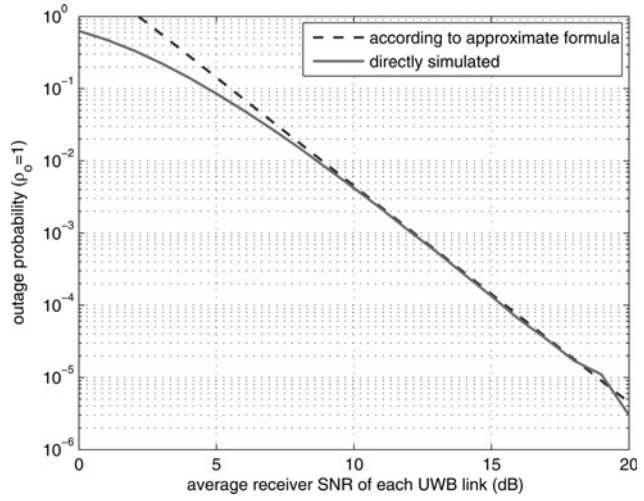

Figure 2 *Outage probability of each impulse-based UWB data link working in corresponding fading channel: comparison between the two results directly simulated and simulated according to the given approximate formula*

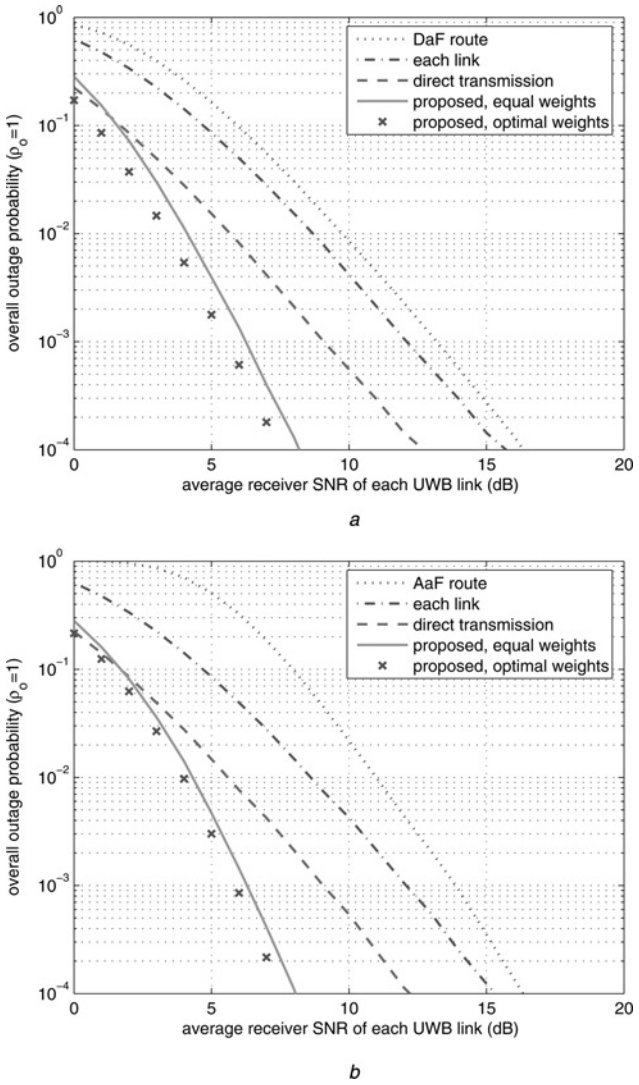

Figure 3 *Outage probabilities of the proposed cooperative beamforming schemes when adopting*

a DaF policy
b AaF policy

doi: 10.1049/iet-com:20080058

policy without any direct transmission; 'AaF route' refers to the route from the source to the destination via the relay adopting the AaF policy without any direct transmission; 'direct transmission' refers to the direct route including the direct transmissions in both the timeslots. We can see that the proposed decentralised cooperative beamforming scheme with equal weights for the relay and the source is very close to the ideal cooperative beamforming scheme with the optimum weights.

The source codes using MatLab are available on request from the corresponding author.

6 Conclusion

In this paper, we have investigated the impacts of promising UWB data links, mainly the more likely adopted impulse-based UWB data links for low data rate applications, on the extensively developed cooperative wireless *ad hoc* networks, taking the three-node relay network as an example. We first investigated the diversity order of data transfer of each impulse-based UWB data link working in the corresponding fading channel and gave the approximate relationship between the diversity order and the channel model parameters, and then proposed and investigated efficient cooperative and decentralised diversity schemes that can utilise the widely spread and independently distributed multiple paths of the fading UWB channels. Performance analysis and simulation studies show that the proposed decentralised cooperative beamforming schemes can achieve full diversity and are more efficient than their decentralised cooperative routing counterparts.

7 Acknowledgments

This work was supported by the EU-funded PULSERS research project.

8 References

[1] MURTHY C.S.R., MANOJ B.S.: 'Ad-hoc wireless networks: architectures and protocols' (Prentice Hall, 2004)

[2] LANEMAN J.N., TSE D.N.C., WORNELL G.W.: 'Cooperative diversity in wireless networks: efficient protocols and outage behavior', *IEEE Trans. Inf. Theory*, 2004, **50**, (12), pp. 3062–3080

[3] AZARIAN K., GAMAL H.E., SCHNITER P.: 'On the achievable diversity-multiplexing tradeoff in half-duplex cooperative channels', *IEEE Trans. Inf. Theory*, 2005, **51**, (12), pp. 4152–4172

[4] http://www.uwbforum.org, the website for the UWB Forum, accessed 2007

[5] PORCINO D., HIRT W.: 'Ultra-wideband radio technology: potential and challenges ahead', *IEEE Commun. Mag.*, 2003, **41**, (7), pp. 66–74

[6] http://www.pulsers.eu, the website for the EU funded PULSERS research project, accessed 2007

[7] http://www.commsp.ee.ic.ac.uk/wiser/pulsers/, the website for the EU funded PULSERS research project at Imperial College, accessed 2007

[8] QIU R.C., ZHOU C., GUO N., ZHANG J.Q.: 'Time reversal with MISO for ultra-wideband communications: experimental results', *IEEE Antennas Wirel. Propag. Lett.*, 2006, **5**, (1), pp. 269–273

[9] GUO N., SADLER B.M., QIU R.C.: 'Reduced-complexity UWB time reversal techniques and experiemental results', *IEEE Trans. Wirel. Commun.*, 2007, **6**, (12), pp. 4221–4226

[10] SALEH A., VALENZUELA R.A.: 'A statistical model for indoor multipath propagation', *IEEE J. Sel. Areas Commun.*, 1987, **5**, (2), pp. 128–137

[11] QIU R.C.: 'A study of the ultra-wideband wireless propagation channel and optimum UWB receiver design', *IEEE J. Sel. Areas Commun.*, 2002, **20**, (9), pp. 1628–1637

[12] CASSIOLI D., WIN M.Z., MOLISCH A.F.: 'The ultra-wide bandwidth indoor channel: from statistical model to simulations', *IEEE J. Sel. Areas Commun.*, 2002, **20**, (6), pp. 1247–1257

[13] MOLISCH A.F.: 'Ultrawideband propagation channels: theory, measurement, and modeling', *IEEE Trans. Veh. Technol.*, 2005, **54**, (5), pp. 1528–1545

[14] ABOU-RJEILY C., DANIELE N., BELFIORE J.C.: 'On the amplify-and-forward cooperative diversity with time-hopping ultra-wideband communications', *IEEE Trans. Commun.*, 2008, **56**, (4), pp. 630–641

[15] AKCABA C., NABAR R.U., LEUNG K.K.: 'A PHY/MAC approach to wireless routing'. Proc. IEEE ICC 2006, Istanbul, Turkey, June 2006, pp. 4474–4478

[16] BLETSAS A., KHISTI A., REED D.P., LIPPMAN A.: 'A simple cooperative diversity method based on network path selection', *IEEE J. Sel. Areas Commun.*, 2006, **24**, (3), pp. 659–672

[17] ZHU S., LEUNG K.K.: 'Distributed cooperative routing for UWB ad hoc networks'. Proc. IEEE ICC 2007, Glasgow, UK, June 2007, pp. 3339–3344

[18] CHIN W.H., SIVAGAMI A.: 'Transmit beamforming in cooperative networks'. Proc. IEEE Vehicular Technology Conf., 2008, pp. 1365–1368

[19] DING Z., CHIN W.H., LEUNG K.K.: 'Distributed beamforming and power allocation for cooperative networks', *IEEE Trans. Wirel. Commun.*, 2008, **7**, (5), pp. 1817–1822

[20] ZHENG L., TSE D.N.C.: 'Diversity and multiplexing: a fundamental tradeoff in multiple antenna channels', *IEEE Trans. Inf. Theory*, 2003, **49**, (5), pp. 1073–1096

9 Appendix

9.1 Proof of Theorem 1

The receiver SNR of the combined source-destination data transer route is

$$\rho = \begin{cases} \rho_{sd} + \max(\rho_{sd}, \rho_{rd}), & \text{if } \rho_{sr} \geq \rho_o \\ 2\rho_{sd}, & \text{otherwise} \end{cases} \tag{43}$$

and, hence, the corresponding outage probability is

$$\begin{aligned} \Pr\{\rho < \rho_o\} &= \Pr\{\rho_{sr} \geq \rho_o\}\Pr\{\rho_{sd} + \max(\rho_{sd}, \rho_{rd}) < \rho_o\} \\ &\quad + \Pr\{\rho_{sr} < \rho_o\}\Pr\{2\rho_{sd} < \rho_o\} \\ &= \Pr\{\rho_{sr} \geq \rho_o\}\Pr\{2\rho_{sd} < \rho_o\}\Pr\{\rho_{sd} + \rho_{rd} < \rho_o\} \\ &\quad + \Pr\{\rho_{sr} < \rho_o\}\Pr\{\rho_{sd} < \frac{\rho_o}{2}\} \\ &< \Pr\{\rho_{sr} \geq \rho_o\}\Pr\{2\rho_{sd} < \rho_o\}\Pr\{\rho_{rd} < \rho_o\} \\ &\quad + \Pr\{\rho_{sr} < \rho_o\}\Pr\left\{\rho_{sd} < \frac{\rho_o}{2}\right\} \end{aligned} \tag{44}$$

As each of the impulse-based UWB data links exhibits the data transfer AOP $\Omega(\rho_o/\overline{\rho})^{\omega}$, the data transfer AOP of our case is

$$\begin{aligned} P_{out}^{(asy)} &< \frac{\Omega^2}{2^{\omega}}\left(\frac{\rho_o}{\overline{\rho}}\right)^{2\omega} + \frac{\Omega^2}{2^{\omega}}\left(\frac{\rho_o}{\overline{\rho}}\right)^{2\omega} \\ &= \frac{\Omega^2}{2^{\omega-1}}\left(\frac{\rho_o}{\overline{\rho}}\right)^{2\omega} \end{aligned} \tag{45}$$

This proves the theorem. □

9.2 Proof of Theorem 2

The receiver SNR of the combined source-destination data transfer route is

$$\rho = \begin{cases} 1.5\rho_{sd} + 0.5\rho_{rd}, & \text{if } \rho_{sr} \geq \rho_o \\ 1.5\rho_{sd}, & \text{otherwise} \end{cases} \tag{46}$$

and, hence, the corresponding outage probability is

$$\begin{aligned} \Pr\{\rho < \rho_o\} &= \Pr\{\rho_{sr} \geq \rho_o\}\Pr\{1.5\rho_{sd} + 0.5\rho_{rd} < \rho_o\} \\ &\quad + \Pr\{\rho_{sr} < \rho_o\}\Pr\{1.5\rho_{sd} < \rho_o\} \\ &= \Pr\{\rho_{sr} \geq \rho_o\}\Pr\{3\rho_{sd} + \rho_{rd} < 2\rho_o\} \\ &\quad + \Pr\{\rho_{sr} < \rho_o\}\Pr\left\{\rho_{sd} < \frac{\rho_o}{1.5}\right\} \end{aligned} \tag{47}$$

and

$$\Pr\{3\rho_{sd} + \rho_{rd} < 2\rho_o\} \leq \Pr\{3\rho_{sd} < 2\rho_o\}\Pr\{\rho_{rd} < 2\rho_o\} \tag{48}$$

As each of the impulse-based UWB data links exhibits the data transfer AOP $\Omega(\rho_o/\overline{\rho})^{\omega}$, the data transfer AOP of our case is

$$\begin{aligned} P_{out}^{(asy)} &\leq \Omega^2\left(\frac{4}{3}\right)^{\omega}\left(\frac{\rho_o}{\overline{\rho}}\right)^{2\omega} + \frac{\Omega^2}{1.5^{\omega}}\left(\frac{\rho_o}{\overline{\rho}}\right)^{2\omega} \\ &= \frac{4^{\omega} + 2^{\omega}}{3^{\omega}}\Omega^2\left(\frac{\rho_o}{\overline{\rho}}\right)^{2\omega} \end{aligned} \tag{49}$$

This proves the theorem. □

doi: 10.1049/iet-com:20080058